Acta Cryst. (1996). B52, 576–579

Synchrotron X-ray Electron Density in the Layered LaOCl Structure

E. N. MASLEN,[a] V. A. STRELTSOV,[a]* N. R. STRELTSOVA[a] AND N. ISHIZAWA[b]

[a]*Crystallography Centre, University of Western Australia, Nedlands 6907, Australia, and* [b]*Research Laboratory of Engineering Materials, Tokyo Institute of Technology, 4259 Nagatsuta, Midori-Ku, Yokohama 227, Japan. E-mail: strel@crystal.uwa.edu.au*

(*Received 3 October 1995; accepted 1 March 1996*)

Abstract

The deformation density $\Delta\rho$ in lanthanum oxychloride, LaOCl, has been determined for a small, naturally faced single crystal using 0.7 Å synchrotron X-radiation. Accumulation of electron density in the interlayer region stabilizes the structure that contains layers of positively charged Cl atoms. Space group *P4/nmm*, tetragonal, M_r = 190.36, a = 4.1198 (7), c = 6.883 (2) Å, V = 116.8 (5) Å^3, Z = 2, D_x = 5.411 Mg m^{-3}, $\mu_{0.7}$ = 17.28 mm^{-1}, $F(000)$ = 164, T = 293 K, R = 0.011, wR = 0.011, S = 1.98 (7) for 416 unique reflections.

1. Introduction

The anisotropic physical properties of layer-type compounds originate in quasi-two-dimensional structural characteristics that can be modified by intercalation with metal atoms or other radicals.

Lanthanum oxychloride, LaOCl, provides an effective host lattice for rare-earth activators that fluoresce in the visible spectrum. Layer character in the lanthanide (Ln) containing Ln*OX* series becomes more pronounced on progressing from La towards heavier rare earths and halogen *X* atoms. Among the mixed-anion oxides the PbFCl (matlockite) structure of LaOCl, built up by stacking PbO-type sheets of $(LaO)_n$ with double sheets of n Cl atoms, becomes unstable with respect to the trigonal SmSI structure at ErOCl.

The crystalline heavier halogens Cl_2, Br_2 and I_2 form layered orthorhombic structures. X-ray difference densities $\Delta\rho$ for the Cl double layers in LaOCl can be compared productively with those for solid Cl_2 (Stevens, 1979), for three-dimensional metal chlorides such as K_2PdCl_4 and K_2PdCl_6 (Hester & Maslen, 1995), and for rare-earth sesquioxides measured recently with synchrotron X-ray radiation (Maslen, Streltsov & Ishizawa, 1996).

A $\Delta\rho$ map for LaOCl was evaluated with tube Mo $K\alpha$ X-radiation by Etschmann, Maslen & Streltsova (1993). The present experiment was undertaken to allow tentative deductions from that $\Delta\rho$ image to be established firmly using synchrotron radiation.

2. Experimental

Single crystals of LaOCl were prepared using the Wilke (1964) flux growth technique for high-melting metal oxides by decomposing thermally unstable metal compounds in an alkali salt flux. Thermally unstable $La_2(CO_3)_3$ was filtered off after dissolving La_2O_3 in HCl, evaporating until powdered $LaCl_3$ remained and adding aqueous Na_2CO_3. A 1/10 $La_2(CO_3)_3$/NaCl mixture in a platinum crucible was placed in a furnace at 1173 K for 30 min, then cooled at 3° h^{-1}. Plate-like LaOCl crystals with maximum dimensions *ca* 35 μm were formed. The specimen selected for X-ray diffraction measurements was bounded by two {001}, four {101}, four {011} and eight {111} faces with dimensions 3.6 × 12.5 × 12.5 × 16.2 μm, respectively, from the crystal centre, indexed and measured using optical and scanning electron Philips SEM505 microscopes.

Diffraction intensities were measured for a reciprocal space sphere, $(\sin\theta/\lambda)_{max}$ = 1.0924 Å^{-1}, $-8 \le h \le 8$, $-8 \le k \le 8$, $-14 \le l \le 14$ using $\omega/2\theta$ scans with 0.7000 (2) Å synchrotron X-rays on the Tsukuba Photon Factory BL14A four-circle diffractometer (Satow & Iitaka, 1989). Experimental conditions, data processing and computer program systems were as described by Maslen, Streltsov & Ishizawa (1996). Synchrotron intensities with peak count rates exceeding 80 000 c.p.s. were reduced by Au foils with an attenuation factor 26.46. Experimental and refinement details are set out in Table 1.*

The lattice constants, evaluated from diffractometer angles for ±(800), ±(080), ±(00,14) reflections at 2θ = 85.64, 85.64 and 90.78°, respectively, are consistent with Brixner & Moore (1983). The linear absorption coefficient μ for analytical absorption correction was evaluated from atomic absorption coefficients at 0.7 Å (Creagh, 1992). The independent atom model (IAM) was the reference state for all structure-factor calculations.

* A list of structure factors has been deposited with the IUCr (Reference: AS0704). Copies may be obtained through The Managing Editor, International Union of Crystallography, 5 Abbey Square, Chester CH1 2HU, England.

Table 1. *Experimental and refinement data for LaOCl*

Diffractometer	PF†
Monochromator	Si(111)
Scan speed (° min^{-1})	16
Peak scan width [$a + b \tan\theta$] (°)	0.45; 0.20
Maximum 2θ (°)	99.76
Max. intensity variation (%) of standards (*hkl*)	5.0 ±(400), ±(040), ±(002)
Reflections measured	4997
Independent reflections	416
Transmission range minimum; maximum	0.654; 0.860
Extinction,‡ r^*	0.17 (8) × 10^3
Minimum extinction *y*§	0.99
R_{int} (F^2)	
Before	0.057
After absorption	0.040
After extinction applied	0.039
R	0.011
wR	0.011
S	1.98 (7)
$(\Delta/\sigma)_{max}$	0.3 × 10^{-3}
$\Delta\rho_{min}$ (e Å^{-3})	−1.09
$\Delta\rho_{max}$ (e Å^{-3})	+1.46
Extinction,¶ r^*	0.2 (1) × 10^3
Minimum extinction *y*§	0.99
R	0.011
wR	0.012
S	2.19 (8)
$(\Delta/\sigma)_{max}$	0.4 × 10^{-4}
$\Delta\rho_{min}$ (e Å^{-3})	−1.13
$\Delta\rho_{max}$ (e Å^{-3})	+1.46
$\sigma(\Delta\rho)$†† (e Å^{-3})	0.20

† The BL14A four-circle diffractometer (Satow & Iitaka, 1989) at the Tsukuba Photon Factory, Japan. ‡ As proposed by Maslen & Spadaccini (1993). § $F_o = yF_{kin}$, where F_{kin} is the value of the kinematic structure factor. ¶ Zachariasen (1967) extinction corrections included in least-squares structure refinement (Larson, 1970). †† Mean e.s.d. (Cruickshank, 1949).

Spherical atom scattering factors were from *International Tables for X-ray Crystallography* (1974, Vol. IV) and dispersion corrections Δf, $\Delta f'$ of −0.309, 2.397 for La, 0.011, 0.006 for O and 0.119, 0.155 for Cl at λ = 0.7 Å were by Creagh (1992).

Before refining the structure, extinction corrections for the full data set were determined from intensities of symmetry-equivalent reflections with different path lengths (Maslen & Spadaccini, 1993). The Zachariasen (1967) extinction parameter r^* (Table 1) indicates limited extinction. Nine independent parameters, including the anisotropic vibration tensor elements, were refined by full-matrix least-squares based on $|F|$ with all measured structure factors weighted by $1/\sigma^2(F_o)$. Atomic charges and the $\Delta\rho$ maps described below were based on this refinement.

The Maslen & Spadaccini (1993) r^* is close to that optimized as part of the least-squares structure refinement (Larson, 1970). The $\Delta\rho$ maps for the alternative refinements were almost identical. The distribution of weighted differences between observed data and model predictions in the least-squares procedure was close to normal, with approximately unit variances satisfying the Gauss–Markov theorem. The least-squares estimation of extinction parameters is therefore unbiased.

Table 2. *Fractional coordinates, anisotropic vibration parameters (U_{ij}, Å^2) and some interatomic distances (Å) with e.s.d.'s in parentheses for LaOCl*

The temperature factor has the expression $T = \exp[-2\pi^2(U_{11}(ha^*)^2 + \ldots + 2U_{12}ha^*kb^* + \ldots)]$.

La on 2 (*c*)	*z*	0.17558 (1)	(4) La—O	2.3883 (3)
$(\frac{1}{4}, \frac{1}{4}, z)$	U_{11}	0.00518 (2)	(1) La—Cl	3.1272 (9)
	U_{33}	0.00628 (3)	(4) La—Cl^{i}	3.2061 (4)
Cl on 2 (*c*)	*z*	0.62991 (9)	(1) La—Cl^{ii}	3.756 (1)
$(\frac{1}{4}, \frac{1}{4}, z)$	U_{11}	0.0128 (1)	(4) La—La^{iii}	3.7853 (4)
	U_{33}	0.0098 (2)	(4) O—O^{iii}	2.9131 (4)
O on 2 (*a*)	U_{11}	0.0062 (2)	(4) O—Cl^{i}	3.2760 (7)
$(\frac{3}{4}, \frac{1}{4}, 0)$	U_{33}	0.0081 (4)	(4) Cl—Cl^{i}	3.4183 (7)
			(4) Cl—Cl^{iv}	4.1198 (7)

Symmetry codes: (i) $\frac{1}{2}+x, -y, 1-z$; (ii) $x, y, z-1$; (iii) $\frac{1}{2}+x, -y, -z$; (iv) $x+1, y, z$.

3. Structure and atomic vibrations

Fractional coordinates and interatomic distances for LaOCl from this synchrotron study listed in Table 2 are within 2 e.s.d's of the less accurate values reported by Brixner & Moore (1983) and Etschmann, Maslen & Streltsova (1993) using X-ray tube single-crystal data.

In the tetragonal unit cell for LaOCl, LaO layers alternate with double Cl layers. Each Cl atom is opposite a La cation in the adjacent sheet. The cation thus acquires 4O + 4Cl + Cl neighbours defining a monocapped square antiprism (Fig. 1). The Cl—Cl^{i} distance between neutral O—La—Cl sandwiches in Table 2 is too short to be of the simple van der Waals type expected for true layer compounds. Although the Cl ion's van der Waals diameter is *ca* 3.62 Å, crystalline Cl_2 also forms an improper layer-type structure containing a *ca* 3.27 Å long intermolecular contact. Strong interaction

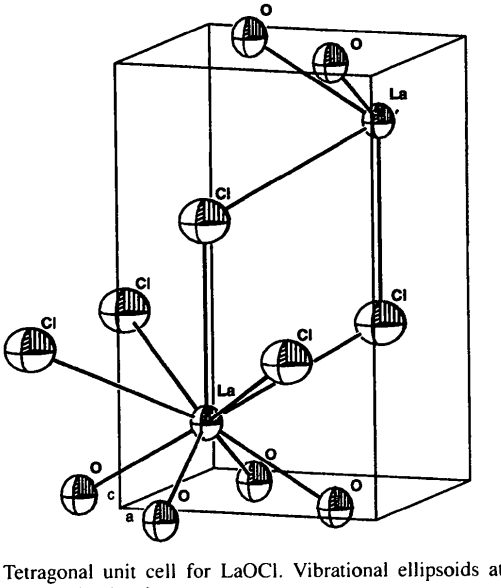

Fig. 1. Tetragonal unit cell for LaOCl. Vibrational ellipsoids at the 99% probability level.

is expected in such structures along non-bonded vectors shorter than the van der Waals separation, as reported for Cl-containing compounds by Hester & Maslen (1995).

The U_{ij} tensor elements for La in Table 2 are slightly smaller and the Cl and O values are within 2 and 1 e.s.d.'s of those reported by Etschmann, Maslen & Streltsova (1993). These authors report e.s.d.'s larger than the values for the present study, due to the lower precision and limited resolution of their Mo $K\alpha$ tube experiments. Comparison with the isotropic vibration parameters for the Cl and O atoms by Brixner & Moore (1983), who measured only 87 independent reflections with $2\theta < 55°$, is of limited value. Whereas both La and O vibrate predominantly along the c axis, the Cl atoms vibrate maximally perpendicular to the c direction, *i.e.* within the Cl layers. This flattening of the Cl-atom vibration ellipsoids along the [001] direction is due to the close packing of the double Cl layers indicated by the short interlayer Cl—Cl contact.

4. Atomic charges and electron density

Atomic charges of La +0.1 (1), O −1.2 (1) and Cl +1.1 (1) e determined by projecting $\Delta\rho$ onto atomic density basis functions (Hirshfeld, 1977) are broadly consistent with La −0.1 (1), O −0.4 (1) and Cl +0.5 (1) e derived from tube data by Etschmann, Maslen & Streltsova (1993), but the synchrotron structure is more polar. Whereas the La atom is almost neutral within the e.s.d., the substantial positive Cl charge contrasts with a negative value expected from electronegativities. Structural stability demands that any negative charge on the Cl atom be small, to avoid strong repulsion between neighbouring Cl layers. Repulsion between positively charged Cl atoms could be counterbalanced by attraction to electron density accumulation between the Cl layers.

The Cl atom in LaOCl packs tightly with its Cl neighbours. Small positive charges also observed on the Cl atom in K_2PdCl_4 (Hester & Maslen, 1995) follow a consistent trend for positive charges to develop on tightly packed atoms in crystals.

The Fig. 2(*a*) $\Delta\rho$ section passes through the La, Cl and O nuclei. Fig. 2(*b*) is perpendicular to the c axis and passes through the Cl layer. The 0.25 e Å^{-3} contour interval exceeds $\sigma(\Delta\rho)$ listed in Table 1. Although the Etschmann, Maslen & Streltsova (1993) map is similar, differences in detail occur due to the limited statistical precision of the tube radiation experiment.

The topographical character of the $\Delta\rho$ maps for the Cl and O layers with their electron concentration near O and depletion near the Cl atoms accounts for the negative and positive charges, respectively, for these atoms. The $\Delta\rho$ depletion near the Cl atoms along the Cl—Cl contacts resembles that in K_2PdCl_4 and K_2PdCl_6 (Hester & Maslen, 1995). The $\Delta\rho$ near the O atoms in Fig. 2(*a*) is not depleted because the O atoms overlap less strongly, resembling more closely the electronegative F anion in K_2SiF_6 (Hester & Maslen, 1995, Fig. 4*b*).

In the La layer (not shown) the $\Delta\rho$ map is depleted, with slight accumulation only in some interatomic regions. In Fig. 2(*a*) electrons accumulate strongly along the [001] direction near the La atoms. Twin

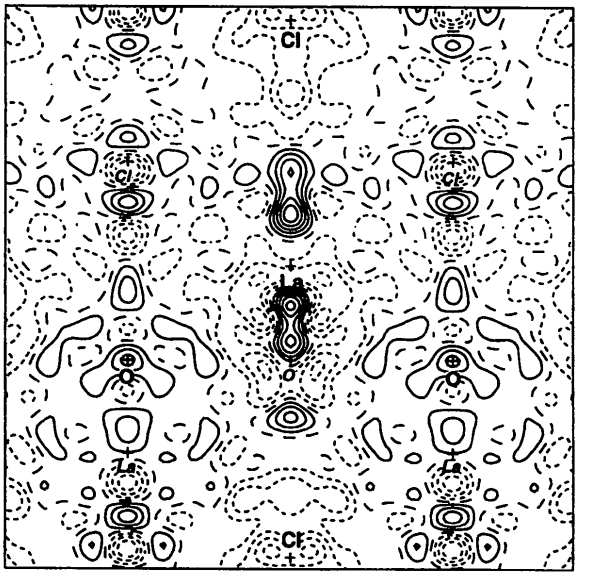

(*a*)

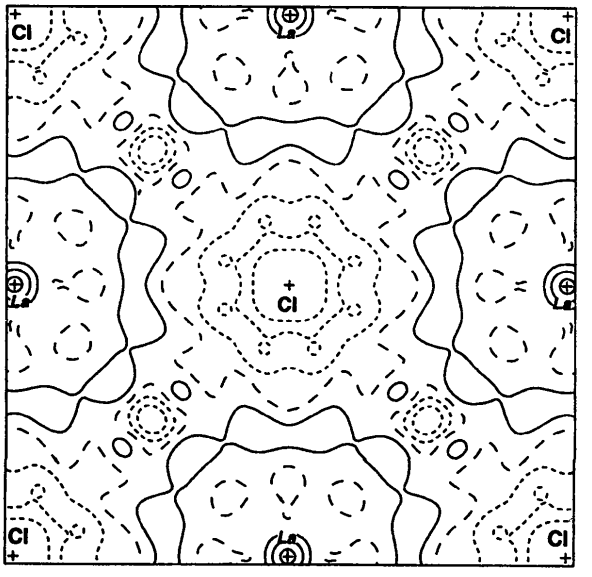

(*b*)

Fig. 2. $\Delta\rho$ for LaOCl in the plane (*a*) through La, O and Cl atoms with the c axis up the map and (*b*) through the Cl layer. The atoms deviating from plane *a* by ±2.06 Å and from plane *b* by −1.34 Å are shown in italics. Map borders 7.2 × 7.2 and 6.0 × 6.0 Å; contour interval 0.25 e Å^{-3}; positive, negative contours – solid, short dashes, respectively.

$\Delta\rho$ density peaks along the –Cl–La–Cl– lines near the La atom are polarized towards the Cl and O layers, indicating that electrons repelled in non-bonding interactions accumulate in the structural cavities within these layers, directly opposite Cl atoms in adjacent layers. The structural cavities in Fig. 2(*b*) are surrounded by circles of positive density. The La positions projected onto Fig. 2(*b*) are -1.34 Å from the plane. Electrons are moved further from the Cl nuclei by exchange interaction within the layers of Cl atoms. The locations of the strong accumulations of electrons are such as to stabilize the structure against repulsion between neighbouring positively charged Cl atoms.

The $\Delta\rho$ in solid Cl_2 (Stevens, 1979) contains doubled peaks along bonding Cl—Cl contacts. Excess non-bonded density towards the back of each Cl atom encircles the Cl—Cl bonds. The electron density near the Cl nuclei in those maps is depleted on the bonding sides and at the mid-point of the Cl—Cl bond. It is also depleted along the short intermolecular contact, emphasizing the importance of exchange, not just in chemical bonds, but also in close non-bonded interactions.

The $\Delta\rho$ topography and other properties for the rare-earth sesquioxides appear to be affected by the electron correlation induced through strong interactions between cations (Maslen, Streltsov & Ishizawa, 1996). Oxygen acts largely as a spacer in those metal oxides, reducing the effective bandwidth for the metal outer electrons and enhancing the effects of correlation. Incorporating the heavier halogens expands the crystal structure sufficiently to reduce the cation–cation interactions. The deformation of the density for LaOCl is characteristic of stronger overlap between halogen anions with saturated bonding capacity.

This work was supported by the Australian Research Council. Financial support of the Australian National Beamline Facility (ANBF) is also acknowledged. The ANBF is funded by a consortium comprising the ARC, DITARD, ANSTO, CSIRO, ANU and UNSW.

References

Brixner, L. H. & Moore, E. P. (1983). *Acta Cryst.* C**39**, 1316.
Creagh, D. C. (1992). Private communication.
Cruickshank, D. W. (1949). *Acta Cryst.* **2**, 65–82.
Etschmann, B. E., Maslen, E. N. & Streltsova, N. R. (1993). XVI Congress of the International Union of Crystallography (Beijing, China). Collected Abstracts. PS-14.02.14.
Hester, J. R. & Maslen, E. N. (1995). *Acta Cryst.* B**51**, 913–920.
Hirshfeld, F. L. (1977). *Isr. J. Chem.* **16**, 198–201.
Larson, A. C. (1970). *Crystallographic Computing*, edited by F. R. Ahmed, S. R. Hall & C. P. Huber, pp. 291–294. Copenhagen: Munksgaard.
Maslen, E. N. & Spadaccini, N. (1993). *Acta Cryst.* A**49**, 661–667.
Maslen, E. N., Streltsov, V. A. & Ishizawa, N. (1996). *Acta Cryst.* B**52**, 414–422.
Satow, Y. & Iitaka, Y. (1989). *Rev. Sci. Instrum.* **60**, 2390–2393.
Stevens, E. D. (1979). *Mol. Phys.* **37**(1), 27–45.
Wilke, K.-Th. (1964). *Z. Anorg. Allg. Chem.* **330**, 164–169.
Zachariasen, W. H. (1967). *Acta Cryst.* A**23**, 558–564.